

# Spin transfer and current-induced switching in antiferromagnets

Helen V. Gomonay

*National Technical University of Ukraine "KPI"  
ave Peremogy, 37, 03056, Kyiv, Ukraine*

Vadim M. Loktev

*Bogolyubov Institute for Theoretical Physics NAS of Ukraine,  
Metrologichna str. 14-b, 03143, Kyiv, Ukraine*

We present theoretical description of the precessional switching processes induced by simultaneous application of spin-polarized current and external magnetic field to antiferromagnetic component of the "pinned" layer. We found stability ranges of different static and dynamic regimes. We showed the possibility of steady current-induced precession of antiferromagnetic vector with frequency that linearly depends on the bias current. Furthermore, we found an optimal duration of current pulse required for switching between different orientations of antiferromagnetic vector and current and field dependence of switching time. Our results reveal the difference between dynamics of ferro- and antiferromagnets subjected to spin transfer torques.

PACS numbers: 72.25.-b, 72.25.Mk, 75.50.Ee

Keywords: Spin transfer torque, spin-polarized current, antiferromagnet

Spin transfer torque is the torque that is applied by non-equilibrium spin-polarized conduction electrons onto a magnetic layer [1, 2, 3]. This effect creates the ability to switch nanoscale magnetic devices at GHz frequencies and stimulate emission of microwaves by steady electric current [4, 5]. Key elements of the spintronic devices, that enable information coding, control and manipulation by an electric current, are two ferromagnetic layers. The "pinned" layer acts as a polarizer for conduction electrons, while the state of "free" layer may be altered by spin transfer torque. However, recent experiments [6, 7, 8, 9, 10] clearly demonstrate that spin-polarized current may also influence the state of another, generally accessory, element – an antiferromagnetic layer, which is used for "pinning". The characteristic value of current density at which switching of antiferromagnetic state takes place varies from  $10^5$  A/cm<sup>2</sup> to  $10^8$  A/cm<sup>2</sup> and in fact proves to be much smaller than the critical current density ( $> 10^8$  A/cm<sup>2</sup>) in ferromagnets. On the other hand, the physical mechanism and details of such a non-trivial dynamics are still unclear. Here we present theoretical description of the precessional switching processes induced by simultaneous application of spin-polarized current and external magnetic field to antiferromagnetic component of the "pinned" layer. We found stability ranges of different static and dynamic regimes. We showed the possibility of steady current-induced precession of antiferromagnetic vector with frequency that linearly depends on the bias current. Furthermore, we found an optimal duration of current pulse required for switching between different orientations of antiferromagnetic vector and current and field dependence of switching time. Our results reveal the difference between dynamics of ferro- and antiferromagnets subjected to spin transfer torques. We anticipate our approach to be a

starting point for more comprehensive analysis of multi-layered magnetic systems in the presence of high-density current. For example, joint behaviour of ferro- and antiferromagnetic layers could be analyzed, with account of the exchange bias coupling.

According to Berger [1] and Slonczewski [2, 3], physical mechanism of spin transfer torque (STT) in ferromagnets (FMs) can be explained in the following way. When free electron transverses (or reflects from) an interface between nonmagnetic and ferromagnetic layer, its spin state can be reversed due to exchange interaction with the localized magnetic moments of FM. This process results in rotation of localized moments in a way that ensures conservation of the total spin of the system.

Due to the efforts of several theoretical groups [11, 12, 13, 14] the concept of STT is extended to the systems with *i*) different types of magnetic ordering, including nonuniform and disordered FM; *ii*) different nature of the magnetic ordering and interaction between the charge carriers and spins, i.e., *s-d* exchange in the magnets with localized spins or itinerant magnetism in the transition metals. It also became clear that the phenomena of STT could result from the atomic scale spin dependent scattering (i.e., hopping of conduction electron between the sites with different directions of magnetic moments).

Generalization of the ideas of Berger and Slonczewski to the case of multisublattice materials is not straightforward due to nontrivial character of the magnetic ordering. Particularly, in antiferromagnets (AFMs) the direction of the atomic magnetic moments varies on the length scale of atomic distances leading to zero net magnetization if averaged over a few lattice constants. Nevertheless, the magnetic structure of AFM may be described with the use of a few macroscopic vectors  $\mathbf{M}_k$  (in the simplest case  $k = 1, 2$ ) called sublattice magnetizations (per

unit volume) which are formed due to strong exchange coupling. So, it seems reasonable to assume that while entering AFM, conduction electrons transfer spin angular momentum to each of magnetic sublattices independently (see Fig. 1). Then, the dynamics of AFM may be described by the system of Landau-Lifshitz-Gilbert equations for  $\mathbf{M}_k$  vectors supplemented with the Slonczewski term  $\mathbf{T}_k$  for STT,  $\mathbf{T}_k = \sigma J[\mathbf{M}_k \times [\mathbf{M}_k \times \mathbf{p}_{\text{cur}}]]/M_0$ , where  $J$  is the current spin polarized in the  $\mathbf{p}_{\text{cur}}$  direction,  $|\mathbf{p}_{\text{cur}}| = 1$ , the constant  $\sigma = \varepsilon \hbar \gamma / (2M_0 V e)$  is proportional to the efficiency  $\varepsilon$  of the scattering processes,  $V$  is the volume of AFM region,  $\hbar$  is the Planck constant,  $e$  is the electron charge,  $\gamma$  is the modulus of the gyromagnetic ratio, and  $M_0 = |\mathbf{M}_k|$  is the saturation magnetization which is supposed to be unchanged under external fields. Positive current value ( $J > 0$ ) corresponds to injection of magnetic moment into AFM layer.

We considered a pinned layer (Fig. 1 a) of a typical exchanged-bias spin valve which includes rather thin AFM layer. High current densities are achieved in a small region (10÷100 nm in diameter), in which both FM and AFM layers could be considered as a single domain. In the case of a moderate pinning the FM works as a spin-polarizer which state is not affected by the precession of AFM vector in the adjacent layer.

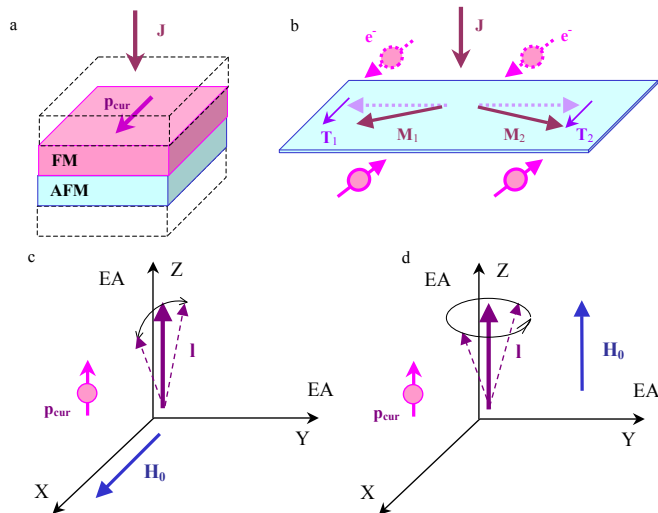


Figure 1: (Color online) **Effect of spin transfer torque within a pinned layer.** a, General structure of a pinned layer. Due to exchange coupling, AFM layer pins the direction of magnetization  $\mathbf{p}_{\text{cur}}$  of the adjacent FM layer. In turns, FM layer polarizes the spin current flowing to AFM. b, Transfer of spin torques  $\mathbf{T}_{1,2}$  from free electrons ( $e^-$ ) to AFM magnetizations  $\mathbf{M}_1$  and  $\mathbf{M}_2$ . Dotted arrows show magnetizations in the absence of current. c, d, Sketch of the eigen modes of AFM vector for different orientations of external magnetic field. Easy axes (EA) are parallel to the film plane.

In our analysis we took into account the fact that AFMs widely used in spintronic devices (FeMn, IrMn) show strong exchange coupling between the different

magnetic sublattices that keeps magnetizations  $\mathbf{M}_1$  and  $\mathbf{M}_2$  almost antiparallel even in the presence of external fields. In this case the state of AFM is described by the only vector order parameter  $\mathbf{l} = \mathbf{M}_1 - \mathbf{M}_2$  (AFM vector), and far below the Néel temperature  $|\mathbf{l}| \approx 2M_0$ . Spin-polarized current and/or external magnetic field induce small tilt of sublattice spins (Fig. 1 b) formally described by macroscopic magnetization  $\mathbf{m} = \mathbf{M}_1 + \mathbf{M}_2$ . Vector  $|\mathbf{m}| \ll |\mathbf{l}|$  is a slave variable that may be excluded from equations of motion.

An effective formalism for investigation of AFM dynamics with the described constraint is based on the use of Lagrange's function (see Supplementary information) deduced in [15] from the Landau-Lifshitz equations. To take into account the effect of STT that can work both as a source or drain of energy for an AFM layer, we deduced the dissipative Rayleigh function

$$\mathcal{R}_{\text{AFM}} = \frac{\alpha_G}{2\gamma M_0} \dot{\mathbf{l}}^2 - \frac{\sigma J}{\gamma M_0} (\mathbf{l}, \dot{\mathbf{l}}, \mathbf{p}_{\text{cur}}). \quad (1)$$

that describes the rate of energy losses in the system,  $\dot{\mathbf{l}}(\partial \mathcal{R}_{\text{AFM}} / \partial \dot{\mathbf{l}}) = -\dot{\mathcal{E}}$ . Here  $\alpha_G$  is a Gilbert damping parameter and  $\mathcal{E}$  is the total energy (per unit volume) of AFM layer.

Analysis of dissipative function (1) shows that STT phenomena in AFM have one general property which is not peculiar to FM. While STT always changes the energy of FM layer, some types of motions in AFM could be nondissipative even in the presence of spin-polarized current. Linearly polarized oscillations of the vector  $\mathbf{l}$ , sketched in Fig. 1c, give an example of nondissipative mode (in neglect of internal damping). And, vice versa, the most effective energy pumping induced by current takes place for any precessional, circular polarized motion of the AFM vector in the plane perpendicular to the direction of current polarization  $\mathbf{p}_{\text{cur}}$  (see Fig. 1d).

To illustrate the peculiarities of non-dissipative and dissipative current-induced dynamics, we analyzed stability of the state with parallel orientation of AFM and FM vectors,  $\mathbf{p}_{\text{cur}} \parallel \mathbf{l}$ , for two different configurations of the external magnetic field  $\mathbf{H}_0$ , depicted schematically in Figs. 1c,d. For the definiteness, AFM layer is supposed to have slightly tetragonal (almost cubic) anisotropy induced by the shape effects or/and interaction with neighboring layers. Two easy axes (Z and Y) are parallel to the film plane.

Configuration with  $\mathbf{p}_{\text{cur}} \parallel \mathbf{l}$  is equilibrium, but not necessarily stable. If free oscillations of AFM vector have circular polarization, any deviation of  $\mathbf{l}$  from the easy axis induced, e.g., by thermal fluctuation, may grow exponentially due to effective pumping by STT.

We found that in the crossed initial orientation,  $\mathbf{H}_0 \perp \mathbf{l}$ , free oscillations have linear polarization below some critical current  $|J| \leq J_{\text{cr}}^{(1)}$ . If the magnetic field is directed along the hard anisotropy axis,  $\mathbf{H}_0 \parallel X$ , vector  $\mathbf{l}$  oscillates within  $XZ$  or  $YZ$  plane (Fig. 1 c) and

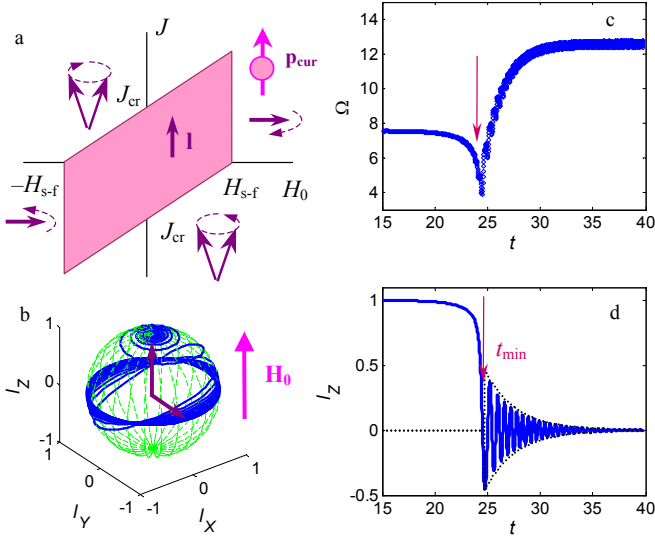


Figure 2: (Color online) **Dynamics of AFM vector induced by steady spin-polarized current.** a, Stability diagram under combined action of field and current. Static state shown with solid arrow is stable within the shaded area. Strong current ( $|J| > J_{\text{cr}}$ ) induces precession of AFM vector around the current polarization  $\mathbf{p}_{\text{cur}}$ , direction of rotation (dashed arrow) depends on the sign of  $J$ . Strong field ( $|H_0| > H_{\text{s-f}}$ ) induces spin flop combined with current-induced precession. b, 3-D evolution of AFM vector  $\mathbf{l}$  in over-critical regime ( $J > J_{\text{cr}}$ ) in the presence of magnetic field  $\mathbf{H}_0$ . In the initial state AFM vector is slightly misaligned from  $Z$  axis. Under the action of STT the vector  $\mathbf{l}$  spirals away from  $Z$  axis with a steadily-increasing precession angle and the angular frequency  $\Omega$ . Final state corresponds to precession with the stable frequency within  $XY$  plane ( $l_z = 0$ ). c, d, Time dependence of the angular frequency  $\Omega$  and  $l_z$  projection. Arrows indicate the moment,  $t_{\text{min}}$ , at which monotonic decrease of  $l_z$  switches to the decaying oscillations. Envelope (dashed line) corresponds to relaxation ( $\propto \exp(-\gamma_{\text{AFM}}t)$ ) caused by internal damping.

$J_{\text{cr}}^{(1)} \equiv \chi_{\perp} |\omega_X^2 - \omega_Y^2 - \omega_H^2| / (2\gamma\sigma M_0)$ . Here  $\chi_{\perp}$  is magnetic susceptibility,  $\omega_{X,Y}$  is the frequency of AFM resonance in the absence of field and current,  $\omega_H = \gamma H_0/2$ . In this case spin torque transferred from the current affects eigen frequencies of spin excitations,  $\Omega_{\pm}^2 = (1/2) \left[ \omega_X^2 + \omega_Y^2 + \omega_H^2 \pm |\omega_X^2 - \omega_Y^2 - \omega_H^2| \sqrt{1 - (J/J_{\text{cr}}^{(1)})^2} \right]$ , but does not affect the effective damping coefficients (as it is the case in FM).

It should be stressed that in the absence of external field the value of critical current depends upon anisotropy of magnetic interactions within and perpendicular to the film plane ( $\omega_X \neq \omega_Y$ ). Magnetic field applied perpendicular to the vector  $\mathbf{l}$  enhances (if  $\mathbf{H}_0$  is parallel to an easy axis) or weakens (if  $\mathbf{H}_0$  is parallel to a hard magnetic axis of AFM) the effective anisotropy. So, magnetic field can be used for control of the critical current. If anisotropy is weak ( $|\omega_X - \omega_Y| \ll \omega_Y$ ), it can be effectively reduced

with the field which value is much less than the spin-flop field  $H_{\text{s-f}} = 4\omega_Y/\gamma$ .

Above the critical current,  $|J| \geq J_{\text{cr}}^{(1)}$ , polarization of free oscillations changes from linear to the circular (elliptic) and STT contributes into the energy dissipation. For one of two modes of free oscillations current-induced pumping competes with the internal damping. Starting from the critical value

$$J_{\text{cr}}^{(2)} \equiv \sqrt{(J_{\text{cr}}^{(1)})^2 + \frac{2\gamma_{\text{AFM}}\chi_{\perp}^2}{\gamma^2 M_0^2 \sigma^2} (\omega_X^2 + \omega_Y^2 + \omega_H^2)}, \quad (2)$$

average energy losses per oscillation period are negative (pumping is greater than damping) and the state with parallel alignment of the current polarization and AFM vectors becomes unstable. Here  $\gamma_{\text{AFM}} \equiv \gamma M_0 \alpha_G / 2\chi_{\perp} \ll \omega_{X,Y}$  is a damping coefficient that can be estimated from the line-width of AFM resonance.

As seen from Eq.(2), the value of critical current  $J_{\text{cr}}^{(2)}$  is independent on the directions of current, field and spin polarization ( $\mathbf{p}_{\text{curr}}$ ), in contrast to the threshold current for FM.

Another type of dynamics is observed in the case when the field is applied parallel to  $\mathbf{l}$  (Fig. 1d). In this case polarization of eigen modes is circular (or elliptic) even for  $J = 0$ . So, oscillations of  $\mathbf{l}$  can actively take up an energy from the current and STT affects damping coefficient, not the frequency of oscillations. Instability point is attained as soon as spin-polarized current overcomes the effect of internal friction.

Fig. 2a shows corresponding dynamical stability diagram plotted in the coordinates field-current for isotropic AFM ( $\omega_X = \omega_Y$ ). Within the shaded area  $|J - \gamma\alpha_G H_0/\sigma| \leq \gamma\alpha_G H_{\text{s-f}}/\sigma$ ,  $|H_0| \leq H_{\text{s-f}}$  the static state with  $\mathbf{l} \parallel Z$  is stable. Above the critical value,  $|J| \geq |J_{\text{cr}}|$ , where  $J_{\text{cr}} \equiv \gamma\alpha_G (H_0 + H_{\text{s-f}} \text{sign} J)/\sigma$ , current may keep up a stable rotation of AFM vector around  $\mathbf{p}_{\text{cur}}$  (Fig. 2 b). Sign reversal of STT (resulted from the reversal of either direction of current,  $J \rightarrow -J$ , or direction of polarization,  $\mathbf{p}_{\text{cur}} \rightarrow -\mathbf{p}_{\text{cur}}$ ) gives rise to rotation in opposite direction. If the field value is greater than spin-flop field,  $|H_0| \geq H_{\text{s-f}}$ , the state with  $\mathbf{l} \parallel \mathbf{H}_0$  is unstable even in the absence of current and in the final state AFM vector is perpendicular to  $\mathbf{H}_0$  and  $\mathbf{p}_{\text{cur}}$ . These results also keep true for nonzero anisotropy.

Some features of the current-induced instability in configuration with  $\mathbf{l} \parallel \mathbf{H}_0$  are similar to those observed in FM. First, in both cases stability region is defined by internal friction which stands up against current-induced rotations [16]. Second, the value of critical current linearly depends on the field [17]. On the other hand, there is still one principal difference that can be detected experimentally. While stability of FM is sensitive to orientation of spin polarization and current direction, current-induced destabilization of AFM takes place for any direction of  $J$  and  $\mathbf{p}_{\text{cur}}$ . Application of the magnetic field results in

variation of the critical current and opens a possibility to reduce  $J_{\text{cr}}$ , as seen from Fig. 2a.

FM layer subjected to the direct spin-polarized current shows one interesting effect – stable precession of the magnetization with the angular frequency close to the frequency of spin-wave mode [4, 5]. To find out whether such an effect could be observed in AFM, we considered in details the dynamics of AFM vector in overcritical regime ( $|J| > |J_{\text{cr}}|$ ) assuming that  $\mathbf{p}_{\text{cur}} \parallel \mathbf{H}_0 \parallel Z$ .

Fig. 2 b shows a typical trajectory of AFM vector (normalized to a unit length) in the presence of steady current  $J = 2.5J_{\text{cr}} < 0$  and field  $H = 0.2H_{\text{s-f}}$ . For calculations we used the following dimensionless values:  $\omega_X = \omega_Y = 6.28$  and  $\gamma_{\text{AFM}} = 0.314$  (that corresponds to the quality factor 20). Initially (at  $t = 0$ ) AFM vector deflected from equilibrium orientation  $\mathbf{l} \parallel Z$  through the small angle  $\theta_0 = 0.001$  within the  $ZY$  plane. Initial velocity corresponded to that mode of free oscillations which is unstable for the chosen current direction. Time unit equals to the period of free oscillations in the absence of field and current.

With the described initial conditions, the motion of  $\mathbf{l}$  vector starts as a rotation around  $Z$  axis with eigen frequency  $\Omega_0 \equiv \omega_X + \omega_H$  of free oscillations. Due to the energy pumping from STT, an amplitude of oscillations (1 projection on  $XY$  plane) slowly increases with an increment proportional to the offset from the critical current value:

$$\frac{1}{\tau} \equiv \gamma_{\text{AFM}} \frac{|J - J_{\text{cr}}|}{J_{\text{cr}}} \left( 1 + \frac{H_0}{H_{\text{s-f}}} \right). \quad (3)$$

The final state ( $t \rightarrow \infty$ ) corresponds to steady rotation of AFM vector in  $XY$  plane ( $l_Z = 0$ ) with the angular frequency  $\Omega_\infty = (J/J_{\text{cr}})\Omega_0$ . Energy dissipation per period of rotation  $\dot{\mathcal{E}} = 0$  due to the pretty balance between magnetic dumping and current-induced pumping. In analogy with FM, such a precessional state of AFM layer can be a source of spin waves. In contrast to FM, the angular frequency  $\Omega_\infty$  is proportional to the current value.

Figs. 2c, d illustrate time evolution of the rotation frequency  $\Omega$  and the component  $l_Z$  between the initial and final states. Due to nonlinear effects, deflection of  $\mathbf{l}$  from the initial direction is accompanied by decrease of  $\Omega$ . At a certain moment  $t = t_{\text{min}}$  (shown by arrow in Figs. 2 c,d) monotonic decrease of  $l_Z$  changes into decaying oscillations around the average value  $l_Z = 0$ . Relaxation of  $\mathbf{l}$  to  $XY$  plane is due to internal damping and follows the law  $\propto \exp(-\gamma_{\text{AFM}}t)$  (see envelope in Fig. 2 d).

In our simulations of AFM dynamics we found that not only  $l_Z$ , but the rotation frequency  $\Omega$ , energy dissipation rate  $\dot{\mathcal{E}}$  and the effective potential energy averaged over a period of rotation ( $= 2\pi/\Omega$ ) have an extremum at the moment  $t = t_{\text{min}}$ . This means that the system passes through the crossing between two attraction points in the phase space. So, we interpret the time interval  $t_{\text{min}}$

as a switching time between two stable states of AFM layer. While exact value of  $t_{\text{min}}$  is sensitive to the ini-

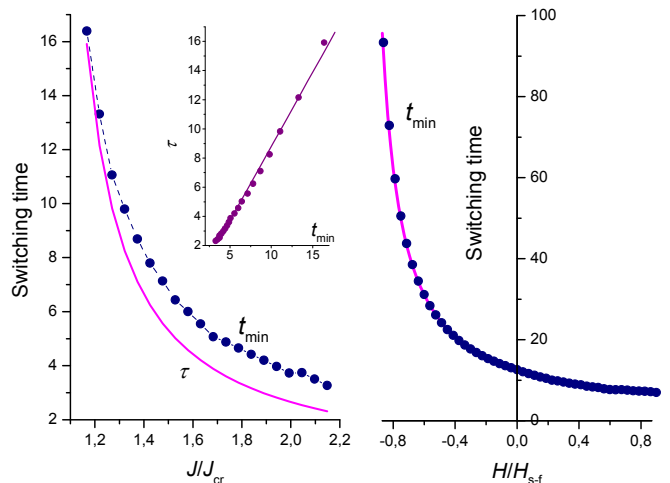


Figure 3: (Color online) **Handling with switching time.** a, Current dependence of calculated switching time,  $t_{\text{min}}$ , and effective pumping coefficient  $\tau \propto |J - J_{\text{cr}}|^{-1}$ , external magnetic field  $H_0 = 0.2H_{\text{s-f}}$  is parallel to  $Z$ . Inset shows correlation between  $\tau$  and  $t_{\text{min}}$  b, Field dependence of switching time  $t_{\text{min}}$  at fixed bias current (points). Solid line shows approximation  $\propto |H_{\text{s-f}} + H_0|^{-1}$ .

tial conditions, it shows the same current (Fig. 3a) and field (Fig. 3b) dependencies as characteristic time  $\tau$  of destabilization (3). Though absolute values of  $t_{\text{min}}$  and  $\tau$  are different, they show good correlation (see inset in Fig. 3 a) in rather wide range of current values. Both values decrease moving far from the stability point  $J_{\text{cr}}$ . This opens the way to diminish the switching time by increasing the current value or by decreasing the critical current with the magnetic field.

From practical point of view it is important to achieve a controllable switching between the different states of AFM (say,  $\mathbf{l} \parallel Z$  and  $\mathbf{l} \perp Z$ ) using current pulses of minimal duration and amplitude. We investigated dynamics of AFM vector under the rectangular current pulses (schematically shown by red line in Fig.4) of different duration and amplitude in overcritical regime ( $J > J_{\text{cr}}$ ). If pulse duration is below  $t_{\text{min}}$ , AFM vector returns back to its initial state after the current is switched off.

Fig. 4 demonstrates switching processes initiated by the current pulse  $J = 2.5J_{\text{cr}}$  with the duration slightly greater than  $t_{\text{min}}$ . The chosen pulse duration ensures maximum deflection of AFM vector from the initial direction as seen from time dependence of  $l_Z$  (Fig. 4 a). After the current is switched off, vector  $\mathbf{l}$  relaxes to the final static state within  $XY$  plane through the damping oscillations during the time  $1/\gamma_{\text{AFM}}$ . Regular rotation around  $Z$  axis supported by current also vanishes with the end of current pulse, as seen from  $\Omega$  behaviour (Fig. 4 b). The final orientation of AFM vector is parallel to one of the easy axes within  $XY$  plane (in the presence of

field, Fig. 4 c) or can be also antiparallel to the initial  $\mathbf{l}$  direction (180° switching) in the absence of external field (Fig. 4 d). Due to degeneracy of the final state, it is very sensitive to the initial conditions and pulse duration and can be predicted only statistically. The results presented

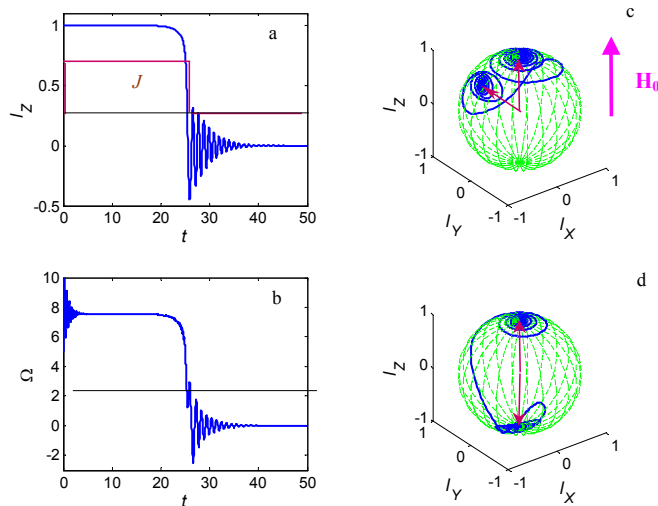


Figure 4: (Color online) **Dynamics of AFM vector induced by a pulse of spin-polarized current.** a, Time dependence of  $l_z$  (blue line) under the rectangular current pulse (red line). Pulse duration close to  $t_{\min}$  is enough to ensure maximal deflection of  $l_z$  from the initial value. b, High frequency rotation of AFM vector persists as long as current induces STT, as seen from time dependence of  $\Omega$ . Just after the current is switched off frequency of rotation goes down to zero and AFM vector lies down to  $XY$  plane. Relaxation time ( $= 1/\gamma_{\text{AFM}}$ ) of both  $\Omega$  and  $l_z$  is due to internal damping. c, Magnetic field applied parallel to initial orientation of  $\mathbf{l}$  induces 90° switching, final state is parallel to  $XY$  plane. d, In isotropic AFM in the absence of field spin-polarized current may induces 180° switching.

here predict direct effect of spin-polarized current on the state of AFM layer usually considered as an accessory element of spin-valves. The described response of AFM vector to electron current may change the properties of the pinned layer. Due to weak but nonzero exchange coupling between AFM and FM layers, reorientation or precession of AFM vector results in variation of the exchange bias field and, consequently, gives rise to the shift of switching fields of spin-valve. Such an effect was observed[7] in nanopillars which included coupled permalloy (FM) and FeMn (AFM) layers. Combined application of the magnetic field and high-density current resulted in an increase of the exchange bias field in this system from

-100 to 100 Oe.

Another evidences of STT effects in AFM could be found from the detailed analysis of the field/current dependence of magnetoresistance, as it was done in Refs. [6, 8, 9, 10]. Magnetoresistance of spin valve should depend on the angle between FM and AFM vectors (in addition to the dependence from mutual orientation of FM vectors in “free” and “pinned” layers) and can change due to the current-induced switching of AFM vector.

The proposed model could be applied to the description of the systems with strong exchange AFM-FM coupling, where behaviour of the pinned layer can be even more curious. Furthermore, it can be extended to non-collinear AFMs with three (like IrMn<sub>3</sub>) and four (like FeMn) magnetic sublattices.

- 
- [1] L. Berger, Phys. Rev. B **54**, 9353 (1996).
  - [2] J. C. Slonczewski, Phys. Rev. B **39**, 6995 (1989).
  - [3] J. Slonczewski, J. Mag. Mag. Mater. **159**, L1 (1996).
  - [4] S. Kaka, M. R. Pufall, W. H. Rippard, T. J. Silva, S. E. Russek, and J. A. Katine, Nature **437**, 389 (2005).
  - [5] A. Slavin and V. Tiberkevich, IEEE Trans. Magn. **45**, 1875 (2009).
  - [6] Z. Wei, A. Sharma, A. S. Nunez, P. M. Haney, R. A. Duine, J. Bass, A. H. MacDonald, and M. Tsoi, Phys. Rev. Lett. **98**, 116603 (2007).
  - [7] S. Urazhdin and N. Anthony, Phys. Rev. Lett. **99**, 046602 (2007).
  - [8] X.-L. Tang, H.-W. Zhang, H. Su, Z.-Y. Zhong, and Y.-L. Jing, Appl. Phys. Lett. **91**, 122504 (2007).
  - [9] N. V. Dai, N. C. Thuan, L. V. Hong, N. X. Phuc, Y. P. Lee, S. A. Wolf, and D. N. H. Nam, Phys. Rev. B **77**, 132406 (2008).
  - [10] J. Bass, A. Sharma, Z. Wei, and M. Tsoi, J. Magn. **13**, 1 (2008).
  - [11] Y. Tserkovnyak, H. J. Skadsem, A. Brataas, and G. E. W. Bauer, Phys. Rev. B **74**, 144405 (2006).
  - [12] A. Nunez, R. Duine, P. Haney, and A. MacDonald, Phys. Rev. B **73**, 214426 (2006).
  - [13] P. M. Haney and A. H. MacDonald, Phys. Rev. Lett. **100**, 196801 (2008).
  - [14] Y. Xu, S. Wang, and K. Xia, Phys. Rev. Lett. **100**, 226602 (2008).
  - [15] I. Bar'yakhtar and B. Ivanov, Sov. J. Low Temp. Phys. **5**, 361 (1979).
  - [16] S. I. Kiselev, J. C. Sankey, I. N. Krivorotov, N. C. Emley, R. J. Schoelkopf, R. A. Buhrman, and D. C. Ralph, Nature **425**, 380 (2003).
  - [17] Y. V. Gulyaev, P. E. Zil'berman, E. M. Epshtein, and R. J. Elliott, JETP **100**, 1005 (2005).